Dynamic Considerations in the Synthesis of Self-Optimizing Control Structures

Michael Baldea
Praxair Technology Center, Praxair Inc., Tonawanda, NY 14150

Antonio Araujo and Sigurd Skogestad
Dept. of Chemical Engineering, Norwegian University of Science and Technology, N-7491 Trondheim, Norway

Prodromos Daoutidis
Dept. of Chemical Engineering and Materials Science, University of Minnesota, Minneapolis, MN 55455

This work builds on our prior results to develop novel control structure design principles for integrated plants featuring multiple time scale dynamics. Specifically, the concept of self-optimizing control can be used to identify the variables that must be controlled to achieve acceptable economic performance during plant operation. This approach does not, however, provide guidelines on control structure design and control loop tuning; a detailed controllability and dynamic analysis is generally needed to this end. In this work, we employ a singular perturbation-based framework, which accounts for the time scale separation present in the open loop dynamics of integrated plants, to identify the available controlled and manipulated variables in each time scale. The resulting controller design procedure thus accounts for both economic optimality and dynamic performance. The developed concepts are subsequently successfully applied on a reactor-separator process with recycle and purge. © 2008 American Institute of Chemical Engineers *AIChE J,* 54: 1830–1841, 2008
Keywords: self-optimizing control, singular perturbations, dynamic analysis

Introduction

Modern chemical plant designs increasingly rely on tight integration between process units, using heat and material recycle streams, to reduce capital and operating costs. In integrated plants, economic gains come, however, at the price of an increased dynamic complexity and control challenges.

The complex dynamic behavior of integrated processes has been characterized in several works.[3,4,5] In particular, integrated processes have long been recognized to exhibit a dynamic behavior that spans multiple time scales. Many

authors[6,7,8,9,10] have indirectly assumed this time scale multiplicity to propose tiered control structures, featuring at least two levels of control action: a primary layer addressing inventory and temperature control at the unit level and providing stability in operation, and a supervisory layer, acting over a slower time scale, that targets the control objectives at the plant level, such as product purity and production rate.

In our previous work,[2] we relied on singular perturbation arguments to rigorously characterize the nonlinear dynamic behavior of integrated processes with large recycle streams and purge streams, demonstrating that it features three time scales, associated, respectively, with the evolution of the states of the individual units, with the evolution of the total material holdup of the network, and with the impurity levels in the network. We derived reduced order nonlinear models

Correspondence concerning this article should be addressed to S. Skogestad at sigurd.skogestad@chemeng.ntnu.no.
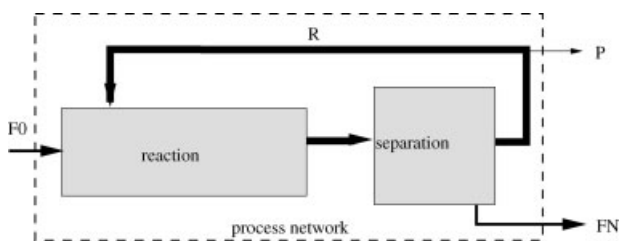
Figure 1. Generic reactor-separator process network with large recycle and purge.

for the dynamics of the process in the three time scales, and our analysis aided in delineating a multitiered controller design framework, using three layers of control action to address objectives, both at the unit and at the network level, using the manipulated inputs identified to be available in each time scale.

Our previous work also addressed the economic issues encountered in the operation of process networks by proposing the concept of self-optimizing control.[1] Specifically, modern plants tend to include optimization and scheduling layers atop the supervisory control system, in order to ensure economic optimality. With this approach, however, economic performance is obtained at the price of computationally expensive real-time optimization calculations. Self-optimizing control[1] aims to alleviate this issued by identifying a set of controlled outputs which, when maintained at their setpoints, ensure that the economic losses affecting the operation of the plant in the presence of disturbances remain at an acceptable level.

This contribution draws on our aforementioned work, utilizing our ideas in[1] to identify the controlled outputs that ensure the near-optimal operation of an integrated process that features multiple time scale dynamics. Self-optimizing control does not, however, provide information concerning the selection of the manipulated inputs to be used to control the desired outputs. In this work, we rely on the analysis in,[2]

which accounts for the time scale separation present in the open loop dynamics of integrated plants, to identify the available controlled and manipulated variables in each time scale. The resulting controller design procedure, thus, accounts for both economic optimality and dynamic performance.

This article is structured as follows: a brief description of self-optimizing control is provided in the next section, succeeded by an account of singular-perturbation based model reduction and controller design. A motivating case study is introduced, and the proposed controller synthesis approach is then presented. Finally, the newly developed framework is demonstrated via simulations.

Self-Optimizing Control

Self-optimizing control[1] is when one can achieve an acceptable loss with constant setpoint values for the controlled variables without the need to reoptimize when disturbances occur (real time optimization).

To quantify this more precisely, we define the (economic) loss L as the difference between the actual value of a given cost function and the truly optimal value, that is

$$L(u, d) = J(u, d) - J_{opt}(d) \qquad (1)$$

Truly optimal operation corresponds to $L = 0$, but in general $L > 0$. A small value of the loss function L is desired as it implies that the plant is operating close to its optimum. The central issue to self-optimizing control is not finding optimal set points, but rather finding the right variables to keep constant. The precise value of an "acceptable" loss varies from case to case, and the selection is made on the basis of engineering and economic considerations.

In[1] we recommended that a controlled variable c suitable for constant set point control (self-optimizing control) should meet the following requirements:

R1. The optimal value of c should be insensitive to disturbances, i.e., $c_{opt}(d)$ depends only weakly on d.
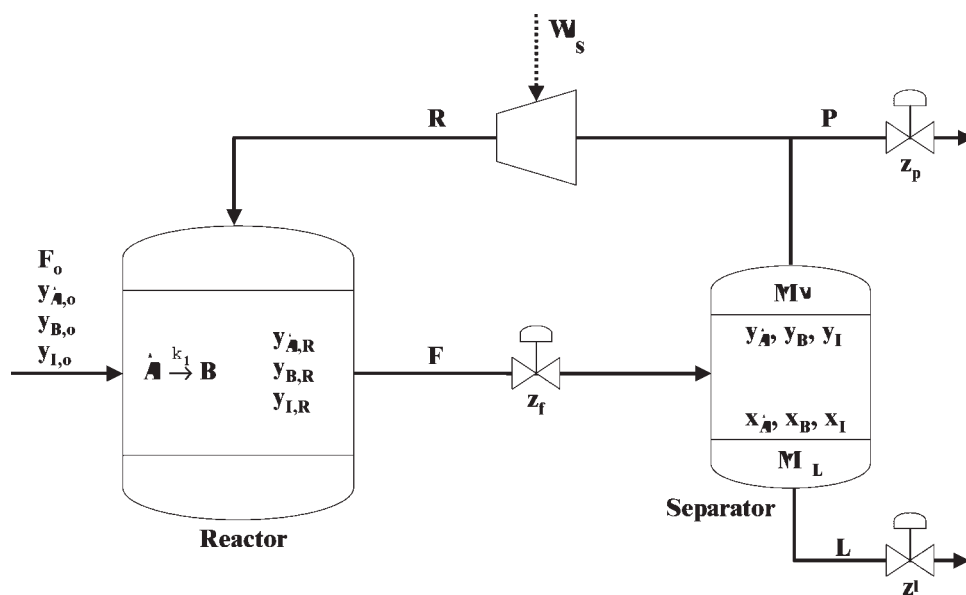

Figure 2. Reactor-separator process.

Table 1. Dynamic Model of the Reactor-Separator with Recycle Network

Differential equations

$$\frac{dM_R}{dt} = F_o + R - F$$

$$\frac{dy_{A,R}}{dt} = \frac{1}{M_R}[F_o(y_{A,o} - y_{A,R}) + R(y_A - y_{A,R}) - k_1 M_R y_{A,R}]$$

$$\frac{dy_{I,R}}{dt} = \frac{1}{M_R}[F_o(y_{I,o} - y_{I,R}) + R(y_I - y_{I,R})]$$

$$\frac{dM_V}{dt} = F - R - N - P$$

$$\frac{dy_A}{dt} = \frac{1}{M_V}[F(y_{A,R} - y_A) - N_A + y_A N]$$

$$\frac{dy_I}{dt} = \frac{1}{M_V}[F(y_{I,R} - y_I) - N_I + y_I N]$$

$$\frac{dM_L}{dt} = N - L$$

$$\frac{dx_A}{dt} = \frac{1}{M_L}[N_A - x_A N]$$

$$\frac{dx_I}{dt} = \frac{1}{M_L}[N_I - x_I N]$$

Algebraic equations

$$P_{\text{reactor}} = \frac{M_R R_{\text{gas}} T_{\text{reactor}}}{V_{\text{reactor}}}$$

$$P_{\text{separator}} = \frac{M_V R_{\text{gas}} T_{\text{separator}}}{\left(V_{\text{separator}} - \frac{M_L}{\rho_L}\right)}$$

$$N_A = K_A \alpha \left(y_A - \frac{P_A^S}{P_{\text{separator}}} x_A\right) \frac{M_L}{\rho_L}$$

$$N_I = K_I \alpha \left(y_I - \frac{P_I^S}{P_{\text{separator}}} x_I\right) \frac{M_L}{\rho_L}$$

$$N_B = K_B \alpha \left[(1 - y_A - y_I) - \frac{P_B^S}{P_{\text{separator}}}(1 - x_A - x_I)\right] \frac{M_L}{\rho_L}$$

$$N = N_A + N_B + N_I$$

$$F = Cv_f z_f \sqrt{P_{\text{reactor}} - P_{\text{separator}}}$$

$$P = Cv_p z_p \sqrt{P_{\text{separator}} - P_{\text{downstream}}}$$

$$R = \frac{W_s}{\frac{1}{\varepsilon} \frac{\gamma R_{\text{gas}} T_{\text{separator}}}{\gamma - 1}\left[\left(\frac{3P_{\text{reactor,max}}}{P_{\text{separator}}}\right)^{\frac{\gamma-1}{\gamma}} - 1\right]}$$

Where:
– M_R, M_V, and M_L denote the molar holdups in the reactor and separator vapor and liquid phases, respectively.
– R_{gas} is the universal gas constant.
– $\gamma = \dfrac{C_P}{C_V}$ is assumed constant.
– Cv_f and Cv_p are the valve constants.
– $P_{\text{downstream}}$ is the pressure downstream the system (assumed constant).
– ε is the compressor efficiency.
– $P_{\text{reactor,max}}$ is the maximum allowed pressure in the reactor.
– The compressor and valves are modeled as first order systems, with time constants $\tau_{\text{compressor}} = 10$ min and $\tau_{\text{valve}} = 1$ min.
– The flowrate L of the liquid product is used to control the separator liquid level.

Table 2. Selected Candidate Controlled Variables

Candidate	Notation
Reactor holdup (Reactor pressure)	P_{reactor}
Vapor mole fraction of A in the reactor	$y_{A,R}$
Vapor mole fraction of I in the reactor	$y_{I,R}$
Vapor mole fraction of A in the separator	y_A
Vapor mole fraction of I in the separator	y_I
Liquid mole fraction of A in the separator	x_A
Liquid mole fraction of I in the separator	x_I
Liquid mole fraction of B in the separator	x_B
Separator pressure	$P_{\text{separator}}$
Flow out of the reactor (Valve opening)	z_F
Liquid flow out of the separator (Valve opening)	z_L
Purge flow (Valve opening)	z_P
Recycle flow	R
Compressor power	W_S

Table 3. Prices for the Components of the Objective Function in (6)

Price	Unit	Value
p_L	\$/mole	2.55
p_P	\$/mole	0.50
p_{F_o}	\$/mole	1.50
p_W	\$/kW	0.08

R2. The value of c should be **sensitive** to changes in the manipulated variable u, i.e., the gain from u to y should be large.

R3. For cases with two or more controlled variables, the selected variables in c should not be closely correlated.

R4. The variable c should be easy to measure and control.

During optimization some constraints are found to be active in which case the variables they are related to must be selected as controlled outputs, since it is optimal to keep them constant at their setpoints (active constraint control). The remaining unconstrained degrees of freedom must be fulfilled by selecting the variables (or combination thereof) which yield the smallest loss L with the active constraints implemented.

Multiple Time Scale Dynamics of Integrated Process Networks

In our previous work,[2] we have demonstrated that the dynamic model of process networks, such as that in Figure 1, featuring a reaction and a separation section that contain a

Table 4. Disturbances to the Process

		Nominal	Disturbance (Δ)
D1	Feed rate (F_o) [mole/min]	100	+20 (+20%)
D2	Feed rate (F_o) [mole/min]	100	−10 (−10%)
D3	Composition of inerts in the feed ($y_{I,o}$)	0.02	+0.004 (+20%)
D4	Product purity (x_B)	0.8711	−0.0436 (−5%)
D5	Product purity (x_B)	0.8711	+0.0436 (+5%)
D6	Composition of product B in the feed ($y_{B,o}$)	0	+0.02†

†Reduction of $y_{A,o}$ by the same amount.

Table 5. Optimization Subject to the Disturbances Considered in Table 4

	Unit	Nominal	D1	D2	D3	D4	D5	D6
Profit	$/min	98.29	116.80	88.84	97.01	98.87	97.18	98.39
M_R	mole	6449	6449	6449	6449	6449	6449	6449
$y_{A,R}$	mole/mole	0.2625	0.3140	0.2366	0.2610	0.2496	0.2751	0.2564
$y_{I,R}$	mole/mole	0.5542	0.5023	0.5803	0.5647	0.5803	0.4970	0.5620
M_V	mole	12.36	12.01	12.32	12.32	12.31	12.30	12.32
y_A	mole/mole	0.2792	0.3323	0.2515	0.2758	0.2620	0.2934	0.2724
y_I	mole/mole	0.6234	0.5518	0.6608	0.6280	0.6730	0.5447	0.6326
M_L	mole	74150	74017	74236	74162	74406	73656	74173
x_B	mole/mole	0.8711	0.8711	0.8711	0.8711	0.8275	0.9147	0.8711
x_A	mole/mole	0.1288	0.1288	0.1288	0.1288	0.1724	0.0853	0.1288
x_I	mole/mole	0.0000557	0.0000527	0.0000555	0.0000555	0.0000554	0.0000551	0.0000554
$P_{reactor}$	Pa	2000000	2000000	2000000	2000000	2000000	2000000	2000000
$P_{separator}$	Pa	540094	453815	599573	546729	770258	340234	553578
N_A	mole/min	12.48	14.91	11.25	12.40	16.74	8.22	12.48
N_I	mole/min	0.03	0.03	0.03	0.03	0.03	0.03	0.03
N_B	mole/min	84.33	100.77	76.04	83.80	80.31	88.14	84.37
N	mole/min	96.84	115.70	87.33	96.23	97.08	96.38	96.89
F	mole/min	871.21	1289.62	716.16	954.74	704.46	1100.46	867.69
L	mole/min	96.84	115.70	87.33	96.23	97.08	96.38	96.89
P	mole/min	3.16	4.30	2.67	3.77	2.92	3.62	3.11
R	mole/min	771.21	1169.62	626.16	854.74	604.46	1000.46	767.69
z_F	–	0.25	0.36	0.20	0.27	0.21	0.30	0.24
z_P	–	0.19	0.31	0.15	0.23	0.12	0.36	0.19
W_S	kW	171.96	291.20	140.37	189.08	105.92	296.32	168.45

recycle loop with the recycle flow rate R, and relying on a purge stream of flow rate P to eliminate any impurities present in small quantities, is captured by a stiff system of equations of the form

$$\frac{d}{dt}\mathbf{x} = \mathbf{f}(\mathbf{x},\mathbf{u}^s) + \frac{1}{\varepsilon_1}\mathbf{G}^l(\mathbf{x})\mathbf{u}^l + \varepsilon_2\mathbf{g}^P(\mathbf{x})u_p \qquad (2)$$

In Eq. 2, $\mathbf{x} \in \mathbb{R}^n$ is the state vector, with $\mathbf{u}^l \in \mathbb{R}^{m^l}$ being the vector of scaled input variables corresponding to the flow rates of the internal streams within the recycle loop, $\mathbf{u}^s \in \mathbb{R}^{m^s}$ being the vector of scaled input variables corresponding to the flow rates of the streams outside the recycle loop (excluding the purge stream), and u_p being a scaled input variable corresponding to the flow rate of the purge stream; $\mathbf{\bar{f}}(\mathbf{x},\mathbf{u}^s)$, $\mathbf{g}^P(\mathbf{x})$ are n-dimensional vector functions, and $\mathbf{G}^l(\mathbf{x})$ is a $n \times m^l$- dimensional matrix.

Equation 2 is developed based on the assumption that the flow rates of the recycle loop streams are are of comparable magnitude, and much higher than the network throughput,

such that, at steady state, we have $\varepsilon_1 = F_{o,s}/R_s \ll 1$, and that, conversely, the flow rate of the purge stream is significantly lower than the network throughput, *i.e.*, $\varepsilon_2 = P_s/F_{o,s} \ll 1$.

Using nested singular perturbation arguments, we demonstrated that the dynamic behavior of the process network in Figure 1 features three components, that evolve over three distinct time scales. Specifically:

• a fast component, evolving in the fast time scale $\tau = t/\varepsilon_1$, described by an equation system of the form

$$\frac{d}{d\tau_1}\mathbf{x} = \mathbf{G}^l(\mathbf{x})\mathbf{u}^l \qquad (3)$$

The "stretched" time scale τ_1 is in the order of magnitude of the time constants of the individual process units with large material throughput that are part of the recycle loop, and thus the model in Eq. 3 effectively captures the dynamics of thes individual process units.

Table 6. Loss Evaluation ($/min) for Selected Candidate Variables Based on Table 2[†]

Candidate	D1	D2	D3	D4	D5	D6	Avg.
$y_{A,R}$	Inf	0.36661	0.02890	0.17707	Inf	0.09963	Inf
$y_{I,R}$	Inf	0.01265	0.00456	0.00939	Inf	0.00199	Inf
y_A	Inf	0.22442	0.01111	0.12012	Inf	0.02979	Inf
y_I	Inf	0.22490	0.01116	0.37894	Inf	0.02979	Inf
x_A	0.00003	0.00000	0.01111	0.57275	Inf	0.02981	Inf
x_I	0.00003	0.00000	0.00000	0.00000	0.00009	0.00004	0.00003
$P_{separator}$	Inf	0.13732	0.01110	0.56009	Inf	0.02906	Inf
R	0.07558	0.00730	0.00263	0.00813	0.02706	0.00005	0.02013
z_F	0.07967	0.00740	0.00266	0.00512	0.02170	0.00007	0.01944
z_P	Inf	0.30234	Inf	0.54822	Inf	0.02980	Inf
W_S	0.13227	0.01391	0.00241	0.03465	0.13660	0.00006	0.05332

[†]Inf means infeasible operation.

Table 7. Control Structure Selection Based on the Singular Perturbation Analysis.

Time scale	Controlled output	Manipulation
Fast	M_R (P_{reactor})	F (z_f)
Fast	M_V ($P_{\text{separator}}$)	R (z_p)
Intermediate	M_L	L
Intermediate	x_b	$M_{R,\text{setpoint}}$ ($P_{\text{reactor,setpoint}}$)
Slow	$y_{I,R}$	P

• an intermediate component, evolving in the time scale t

$$\frac{d}{dt}\mathbf{x} = \tilde{\mathbf{f}}(\mathbf{x}, \mathbf{u}^s) + \varepsilon_2 \tilde{\mathbf{g}}^P(\mathbf{x})u_p$$
$$\mathbf{0} = \tilde{\mathbf{G}}^l(\mathbf{x})\mathbf{u}^l(\mathbf{x}) \tag{4}$$

with $\mathbf{0} = \tilde{\mathbf{G}}^l(\mathbf{x})\mathbf{u}^l(\mathbf{x})$ being the linearly independent constraints that denote the quasi-steady state of the fast dynamics in the time scale t. Equation 4 is a description of the core dynamics of the process network, that is due to the presence of the recycle loop with large recycle flow rate.

• a slow component, evolving in the compressed time scale $\theta = \varepsilon_2 t$, of the general form

$$\frac{d}{d\theta}\mathbf{x} = \hat{\mathbf{g}}^P(\mathbf{x})u_p + \hat{\mathbf{B}}(\mathbf{x})$$
$$\mathbf{0} = \hat{\mathbf{G}}(\mathbf{x})\mathbf{u}^s(\mathbf{x}) \tag{5}$$
$$\mathbf{0} = \tilde{\mathbf{G}}^l(\mathbf{x})\mathbf{u}^l(\mathbf{x})$$

Note that, in Eq. 5, not only the fast dynamics, but also the intermediate dynamics of the network are considered to be at a quasi-steady state. The slow component captures the dynamics associated with the presence of small amounts of feed impurity that are removed by the small purge stream.

Note that description of each of the models of the dynamics in the fast, intermediate, and slow time scales described previously (respectively, Eqs. 3,4,5), features a distinct group

of manipulated inputs (respectively, $\mathbf{u}^l$, $\mathbf{u}^s$ and u_p), that act upon and can be used to address control objectives in the respective time scale.

By way of consequence, process networks featuring significant material recycling, as well as a purge stream for eliminating impurities, lend themselves naturally to a hierarchical control structure, featuring three layers of control action:

• Control objectives at the unit level should be addressed in the fast time scale, using the large flow rates of the internal material streams $\mathbf{u}^l$, as manipulated inputs.

• The control of the network wide objectives (such as product purity and production rate), should be undertaken in the intermediate time scale, using the flow rates $\mathbf{u}^s$ of the material streams outside the recycle loop as manipulated inputs.

• The impurity levels in the network should be regulated using the flow rate u_p of the purge stream, over a long time horizon (slow time scale).

In the following section, we demonstrate how these results, along with the concept of self-optimizing control reviewed earlier, can be successfully fused in a control design procedure that accounts for both economic optimality and dynamic performance.

Case Study on Reactor-Separator with Recycle Process

In this section, we present a case study that considers a reactor-separator network, interconnected via a recycle stream with a large flow rate (compared to the network throughput), and the inert impurities present in the feed are eliminated by purging. The generic process was studied in,[2] and for this article the pressure-flow relations for the flows F, P, and R and economic data were added.

We rely on this representative example to develop and illustrate a hierarchical controller synthesis procedure, that accounts for both the time scale separation in process dynam-
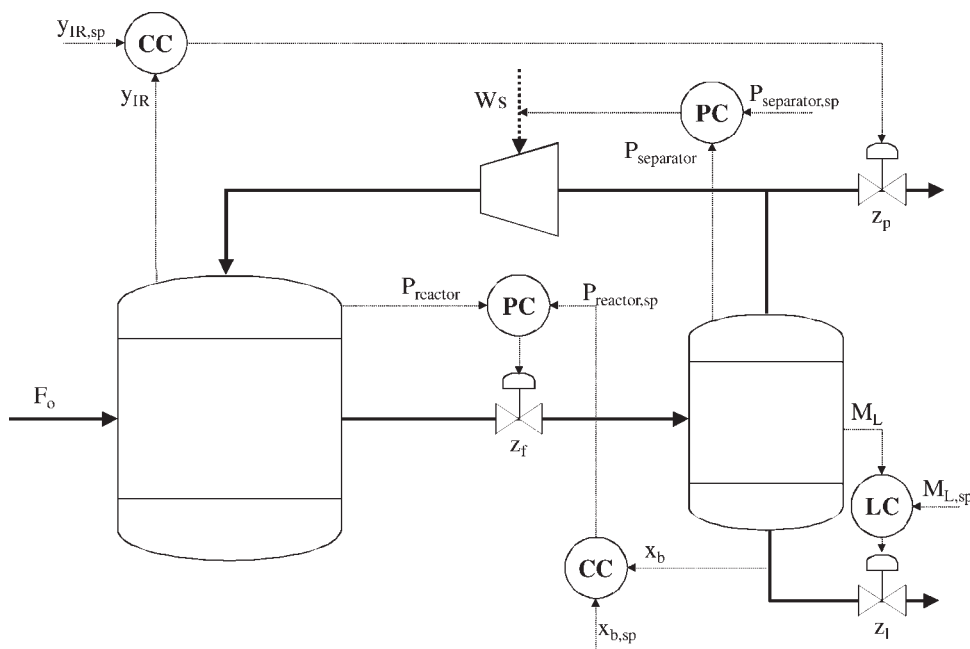

Figure 3. Original configuration based on singular perturbation with control of x_B, $P_{\text{separator}}$, and $y_{I,R}$.
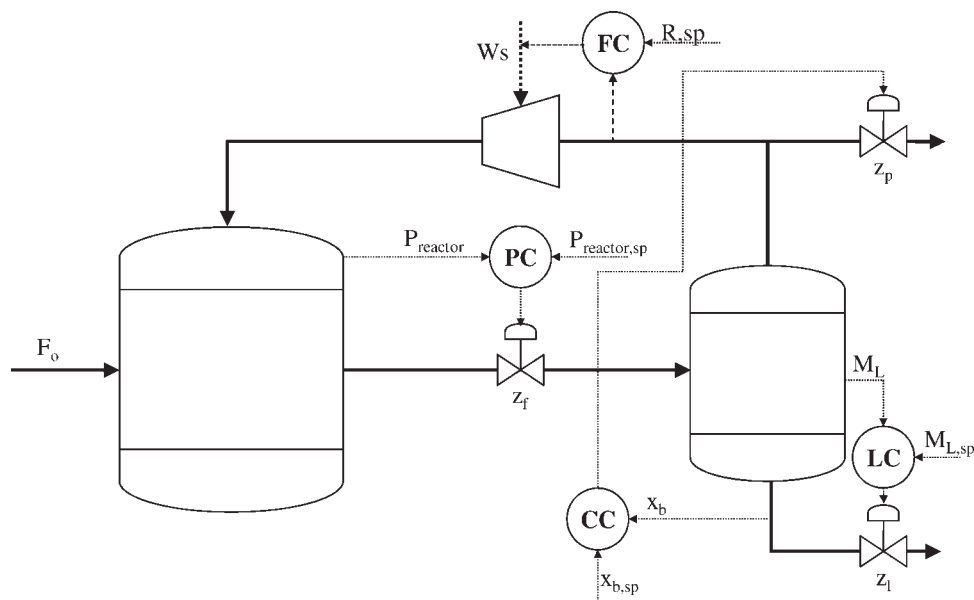
Figure 4. Simplest self-optimizing configuration with control of x_B, $P_{reactor}$, and R.

ics, and for economic criteria, in order to ensure dynamic performance and economic optimality of the closed-loop system.

Process description and modeling

The process consists of a gas-phase reactor and a condenser-separator that are part of a recycle loop (Figure 2). A low single-pass conversion requires that a large (with respect to the feed flow rate) recycle flow rate R be used in order to achieve the desired purity of the product B. The feed stream contains a small amount of an inert, volatile impurity $y_{I,o}$ which is removed via a purge stream of small flow rate P.

The objective is to ensure a stable operation while controlling the purity of the product x_B.

A first-order reaction takes place in the reactor, i.e., $A \xrightarrow{k_1} B$. In the condenser-separator, the interphase mole transfer rates for the components A, B, and I are governed by rate expressions of the form $N_j = K_j \alpha (y_j - \frac{P_j^S}{P} x_j) \frac{M_L}{\rho_L}$, where $K_j \alpha$ represents the mass transfer coefficient, y_j the mole fraction in the gas phase, x_j the mole fraction in the liquid phase, P_j^S the saturation vapor pressure of the component j, P the pressure in the condenser, and ρ_L the liquid density in the separator. A compressor drives the flow from the separator (lower pressure) to
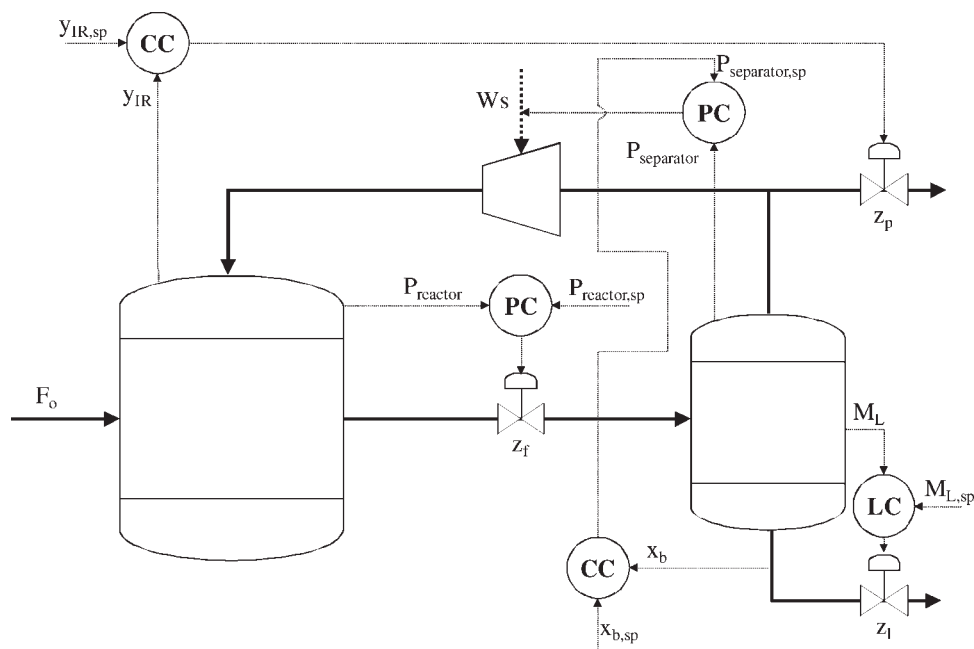

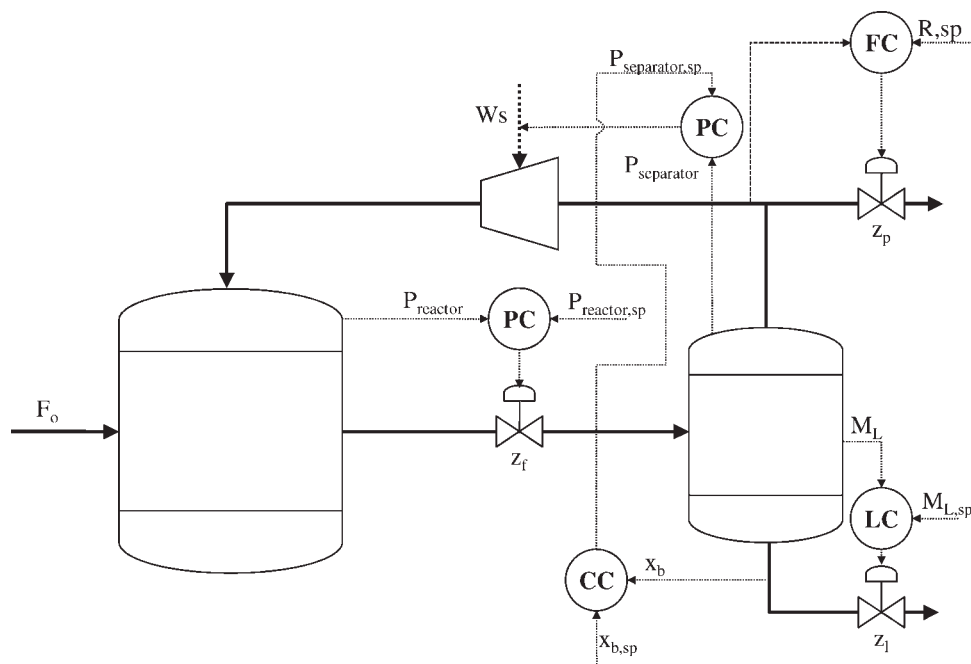**Figure 5. Modification of Figure 3: Constant pressure in the reactor instead of in the separator.**

Figure 6. Final structure from modification of Figure 5: Set recycle flow rate (R) constant instead of the inert composition ($y_{I,R}$).

the reactor. Moreover, valves with openings z_f and z_p allow the flow through F and P, respectively. Assuming isothermal operation (or, equivalently, perfect temperature control), the dynamic model of the system has the form given in Table 1.

Economic approach to the selection of controlled variables: Self-optimizing control computations

Degree of Freedom Analysis. The open loop system has three degrees of freedom at steady state, namely the position of the valve at the outlet of the reactor (z_F), the position of the purge valve (z_P), and the compressor power (W_s).

Table 2 lists the candidate controlled variables considered in this example. With three degrees of freedom and 14 candidate controlled outputs, there are $\binom{14}{3} = \frac{14!}{3!11!} = 364$ possible ways of selecting the control configuration, which constitutes a rather large number if we consider the dimension of the problem. Therefore, in order to avoid evaluation of each one of these possible configurations, we determine whether there are active constraints during operation.

Definition of optimal operation

The following profit is to be maximized

$$(-J) = p_L L + p_P P - p_{F_o} F_o - p_W W_s \qquad (6)$$

subject to

$$
\begin{aligned}
P_{\text{reactor}} &\leq 2000 \; kPa \\
P_{\text{separator}} &\leq 1000 \; kPa \\
x_B &\geq 0.8711 \\
W_S &\leq 300 \; kW \\
z_F, z_P &\in [0,1]
\end{aligned}
\qquad (7)
$$

where p_L, p_P, p_{F_o}, and p_W are the prices of the liquid product L, purge P (here assumed to be sold as fuel), feed F_o, and compressor power W_s, respectively (see also Table 3 for cost-related information).

Identification of important disturbances

We will consider the disturbances and process changes listed in Table 4. Specifically, we account for the possibility of variations in the feed flow rate and composition (including the possibility of having a small quantity of product present in the feed), as well as for possible changes in the product purity requirement.

Optimization

Two constraints are active at the optimum throughout the calculations (each of which corresponds to a different disturbance), namely the reactor pressure P_{reactor}, at its upper bound, and the product purity x_B, at its lower bound (Table 5). These consume two degrees of freedom, since it is optimal to control them at their setpoint,[11] leaving one unconstrained degree of freedom.

Unconstrained variables: Evaluation of the loss

In order to identify the remaining controlled variable, we evaluate the steady-state economic loss incurred in the pres-

Table 8. Final Control Structure Based on Dynamic Analysis and Optimality

Time scale	Controlled output	Manipulation
Fast	M_R (P_{reactor})	F (z_f)
Fast	M_V ($P_{\text{separator}}$)	R (W_s)
Intermediate	M_L	L
Intermediate	x_b	$M_{V,\text{setpoint}}$ ($P_{\text{condenser,setpoint}}$)
Slow	R (W_S)	z_p

Table 9. Controller Tuning Parameters for Each Control Configuration in Figures 3–6

Feedback loop	Figure 3	Figure 4	Figure 5	Figure 6
$M_L \times L$	$K_c = 0.001$	$K_c = 0.001$	$K_c = 0.001$	$K_c = 0.001$
$P_{\text{reactor}} \times z_F$	$K_c = 0.001$	$K_c = 0.001$ $\tau_I = 10$	$K_c = 8$ $\tau_I = 16$	$K_c = 8$ $\tau_I = 16$
$P_{\text{separator}} \times W_S$	$K_c = 0.0013$		$K_c = 0.0013$	$K_c = 1.3 \cdot 10^{-5}$
$R \times z_P$				$K_c = 0.005$ $\tau_I = 1000$
$R \times W_S$		$K_c = 0.01$ $\tau_I = 2$		
$y_{I,R} \times z_P$	$K_c = 10$ $\tau_I = 500$		$K_c = 10$ $\tau_I = 410$	
$x_B \times z_P$		$K_c = 100$ $\tau_I = 1000$		
$x_B \times P_{\text{reactor,sp}}$	$K_c = 8$ $\tau_I = 100$			
$x_B \times P_{\text{separator,sp}}$			$K_c = 4$ $\tau_I = 100$	$K_c = 4$ $\tau_I = 100$

Time constants are in minutes.

ence of disturbances, when the candidate controlled variable, in addition to the two active constraints, is perfectly controlled (i.e., it is kept constant).

Table 6 shows the results of the loss evaluation. We can see that the smallest average loss was found for the liquid mole fraction of inert in the separator (x_I). This was somehow expected since its value is essentially constant through-

out the optimizations shown in Table 5. However, composition measurements have large dead times and are unreliable and, we, therefore, disregard this candidate as the potential self-optimizing variable.

Two other candidates which show smaller average losses are the recycle flow rate R and valve opening z_F, with average losses of 0.02013 and 0.01944 \$/min, respectively. As
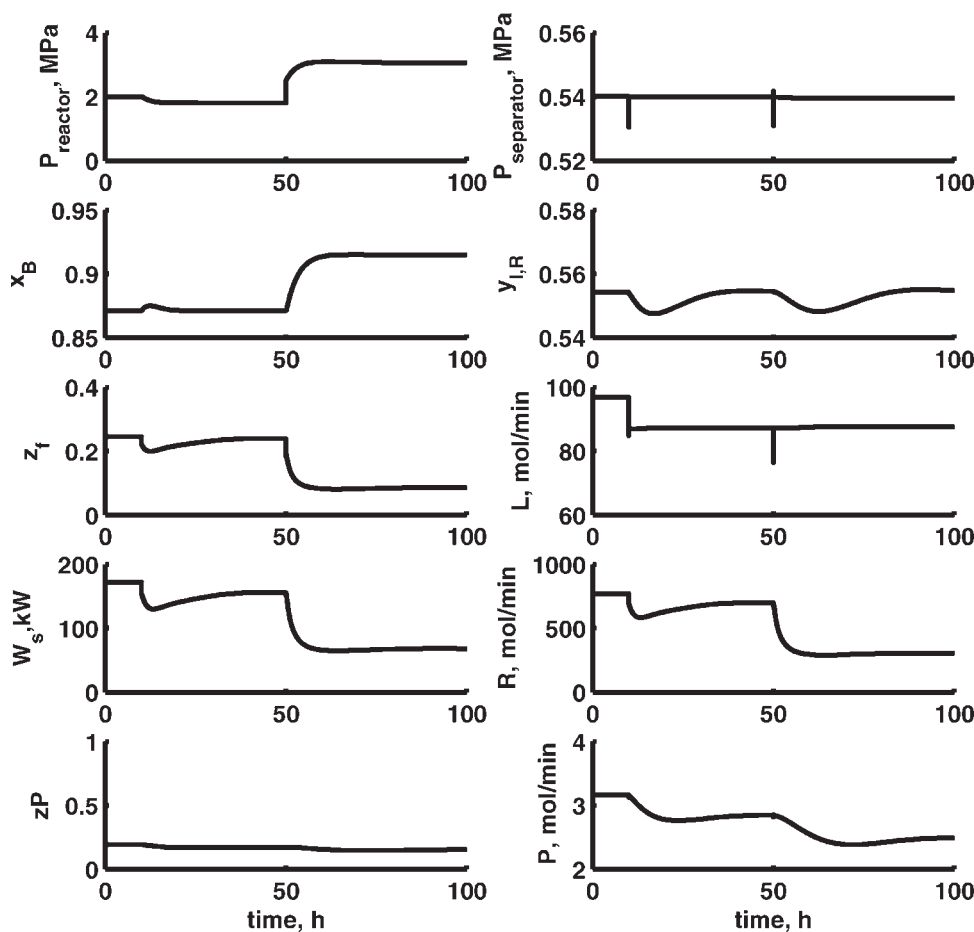

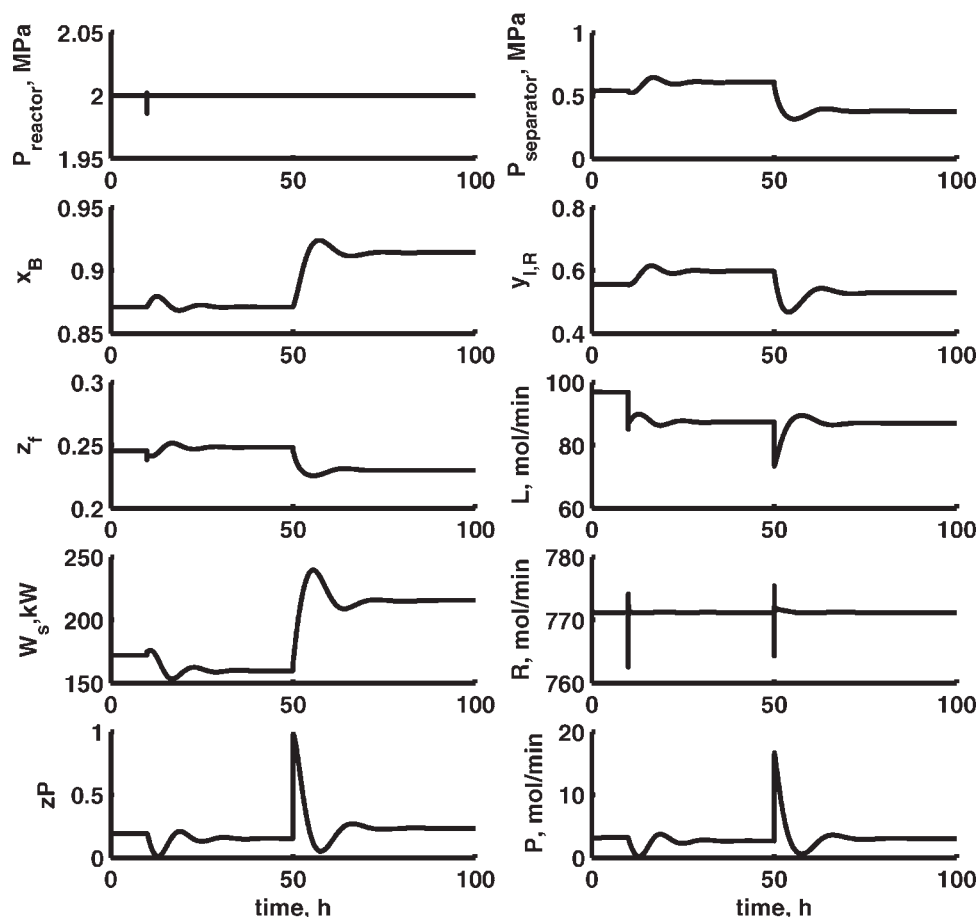Figure 7. Closed-loop responses for configuration in Figure 3.

Figure 8. Closed-loop responses for configuration in Figure 4.

the valve opening z_F is typically required to address the control of the reactor pressure, we select the recycle flow rate R, which has an acceptable loss, as the unconstrained (self-optimizing) controlled variable.

In summary, by the self-optimizing approach, the primary variables to be controlled are then $y = [P_{\text{reactor}} \ x_B \ R]$ with the manipulations $u = [z_F \ z_P \ W_S]$. In addition, secondary controlled variables may be introduced to improve the dynamic behavior of the process. With these variables, a number of control configurations can be assigned and some of them will be assessed later in this article.

Singular Perturbation Approach for the Selection of Controlled Variables

According to the hierarchical control structure design proposed in,[2] based on the time scale separation of the system, the variables to be controlled, and their respective manipulations are given in Table 7.

In the prior work,[2] economics were not a consideration. Moreover, in the aforementioned configuration the reactor pressure is employed to control the purity of the product, and is evidently required and allowed to vary, which could lead, in some cases, to the violation of the operating constraints included in the present problem formulation. A simple modification that allows the pressure constraint in the reactor to be satisfied entails controlling x_B using the separator pres-

sure, while maintaining the reactor pressure at its setpoint. This will be discussed later in this article.

Control Configuration for Optimality and Dynamic Performance

The objective of this study is to explore how the configurations suggested by the two different approaches can be merged to produce an effective control structure for the system. Thus, as a starting point, we employ the following two "original" configurations: Figure 3 presents the original configuration from the singular perturbation approach.[2] Figure 4 depicts the simplest self-optimizing control configuration with control of the active constraints (P_{reactor} and x_B) and self-optimizing variable R.

The configuration in Figure 4 does not account for optimality and could give rise to infeasibility with respect to operating constraints on pressure. On the other hand, the structure outlined in Figure 4 does not directly control the impurity levels in the network, and employs the flow rate of the purge streams to control the product purity, a solution which, according to our previous results, could lead to poor dynamic performance. These observations will be confirmed by the simulation results presented later in this article.

Since one usually starts by designing the regulatory control system, the most natural starting point is the configuration in Figure 3. The first evolution of this configuration is to
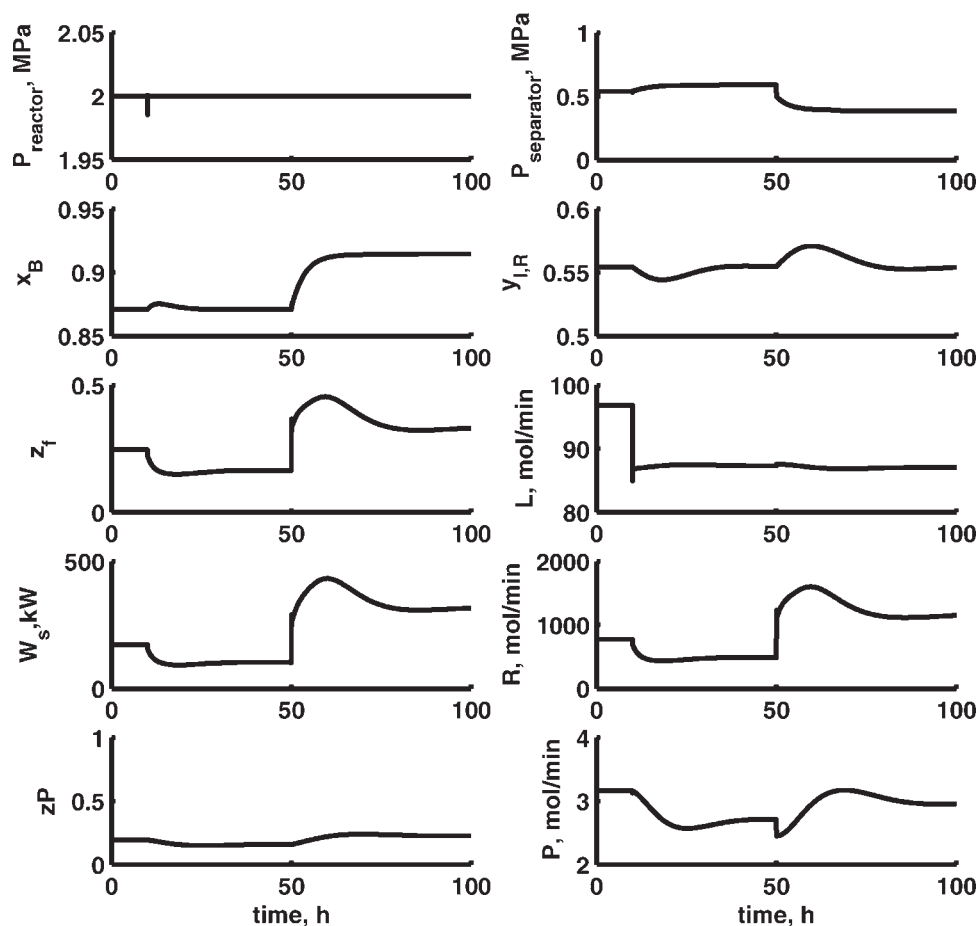
Figure 9. Closed-loop responses for configuration in Figure 5.

change the pressure control from the separator to the reactor (Figure 5). In this case, both active constraints (P_{reactor} and x_B) are controlled in addition to impurity level in the reactor ($y_{I,R}$).

The final modification towards buiding a self-optimizing control structure is to change the primary controlled variable from $y_{I,R}$ to the recycle flow rate R (Figure 6). The latter evolution also ensures that the compressor power is controlled around its steady-state optimal value over a longer time scale, using the flow rate of the purge stream to this end. The final control configuration is summarized in Table 8.

Results and Discussion

Simulations were carried out to assess the dynamic performance of the control configurations proposed earlier. The tuning parameters for the controllers in each configuration are shown in Table 9. The simulation study considered two major disturbances: a 10% drop in the feed flow rate (F_o from 100 to 90 mol/min) at $t = 10$ h followed by a 5% increase in the setpoint for the product purity (x_B from 0.8711 to 0.9147) at $t = 50$ h.

The results are found in Figures 7 through 10.

Based on the aforementioned simulation results presented above, notice that, in the case of the original system in

Figure 3, the reactor pressure rises over the $2MPa$ bound (Figure 7) when a setpoint increase for x_B occurs. The dynamic response in terms of the product purity—a key performance indicator—is, however, very good. Moreover, the aforementioned behavior is to be expected since the original configuration was based on varying the reactor pressure to control the purity of the product.

With P_{reactor} controlled with a controller with integral action (configuration of Figure 5), and manipulating the condenser pressure to control the product purity, a similar dynamic response in x_B is obtained (Figure 9). This is again to be expected, since, as explained earlier, the structures depicted in Figures 3 and 5 are dynamically similar. Note, however, that in this case, tracking the purity setpoint as it increases at $t = 50$ h requires a significant increase in the energy consumption of the compressor (W_S exceeds, in effect, the 300 kW bound imposed in the problem formulation), intuitively leading to a less than optimal profit.

The proposed self-optimizing configuration of Figure 4, whereby the controlled variables are selected based on economics, results in a rather poor dynamic performance for the controlled variable x_B as seen in Figures 8 and 11. The explanation lies in the fact that x_B is controlled by the small flow rate P (using valve position z_P), which leads to a sluggish response. Note also that obtaining a dynamic performance in terms of x_B comparable to that of the aforementioned
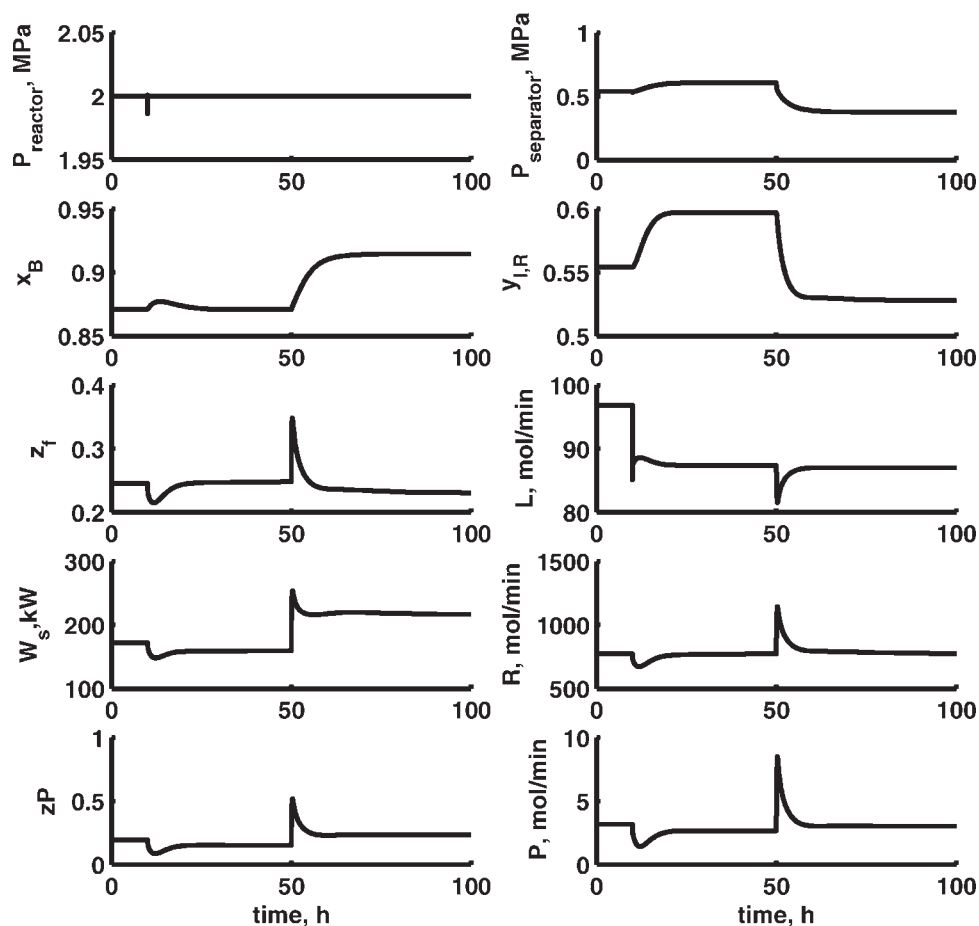
Figure 10. Closed-loop responses for configuration in Figure 6.

configurations entails using a high gain controller. Considering the data in Table 9, the gain of the purity controller in the basic self-optimizing configuration is $K_c = 100$, while the gains of the purity controllers (expressed in terms of

Figure 11. Closed-loop responses for the product purity x_B for the configurations in Figures 3 (solid), 4 (dash), 5 (dot) and 6 (dash-dot).

scaled variables) in the configurations discussed above are, respectively, $K_c = 8$ and $K_c = 4$. As a consequence, in the response of Figure 8, the purge flow P is significantly increased for an extended period of time.

Finally, the configuration in Figure 6 gives feasible operation with a good transient behavior and low compressor energy consumption (Figure 10).

The developments above demonstrate that the approaches proposed in our previous work[1] and[2] are complementary in developing a control configuration at the network level, that is both economically optimal and has good dynamic performance.

The controlled outputs in the configuration illustrated in Figure 6 were selected based on economic considerations, that is, (1) the active constraints in the optimization calculations, and (2) the variables that ensure a minimum loss in the presence of disturbances. The input-output pairings are based on the time scale that each controlled output evolves in, and on the manipulated inputs available in the respective time scale.

Specifically, the pressure changers (valve and compressor) that determine the large internal flowrates are used for the fast regulation of the pressure/holdup in the reactor and condenser vapor phase. Subsequently, the setpoint of the condenser vapor phase pressure controller is used to control the product purity in a slower time scale. Finally, the economic
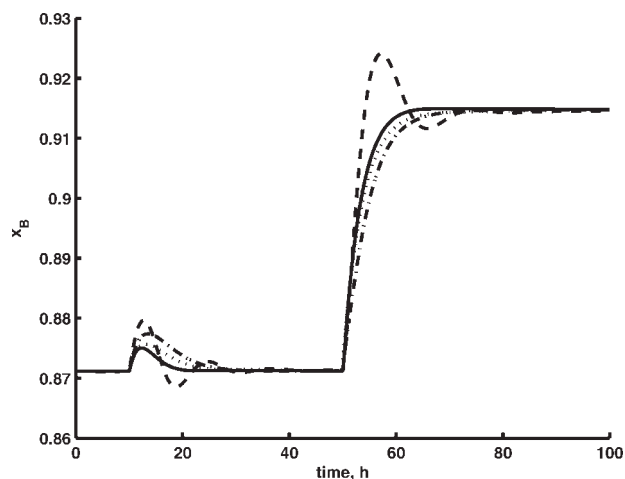
analysis recommends that the original structure be modified in the slow time scale, using the small purge flowrate to regulate the recycle flow at a set value, thereby keeping the compressor power consumption constant.

Notice that the final control structure in Table 8 is not only optimal, but also in complete agreement with the control structure design framework based on singular perturbation analysis (Table 7). Specifically, the control configurations are identical in the fast time scale. Moreover, both the reactor and the condenser pressure setpoints are manipulated inputs acting in the intermediate time scale, with the former being selected in the original configuration (Figure 3) and the latter selected in the final configuration based on optimality considerations. Last, since the flow rate of the recycle stream varies in the intermediate time scale, the purge stream must be used in the slow time scale to reset the recycle flow rate.

Note also that final control configuration proposed earlier is in agreement with Luyben's rule of flow-controlling one of the streams in the recycle loop.[12] However, this rule should be applied with caution.[13]

Conclusion

This work utilized our prior results to develop novel control structure design principles for integrated plants featuring multiple time scale dynamics. Specifically, our concept of self-optimizing control was employed to identify the variables that must be controlled in order to achieve acceptable economic performance during plant operation. This approach does not, however, provide guidelines on control structure design and control loop tuning. We, therefore, relied on our previously introduced singular perturbation-based analysis and control framework, which accounts for the time scale separation present in the open loop dynamics of integrated plants, to identify the available controlled and manipulated variables in each time scale.

Using a prototype reactor-separator process, we successfully demonstrated the development and implementation of a controller design procedure that merges the aforementioned concepts, thereby accounting for both economic optimality and dynamic performance. Numerical simulation results indicated that the resulting control system exhibited very good transient response characteristics, while maintaining the parameters of the system within the desired economic performance envelope.

Literature Cited

1. Skogestad S. Plantwide control: The search for the self-optimizing control structure. *J Proc Contr*. 2000;10:487–507.
2. Baldea M, Daoutidis P. Control of integrated process networks–A multi-time scale perspective. *Comp Chem Eng*. 2007;31:426–444.
3. Mizsey P, Kalmar I. Effects of recycle on control of chemical processes. *Comp Chem Eng*. 1996;20:S883–S888.
4. Contou-Carrére MN, Baldea M, Daoutidis P. Dynamic precompensation and output feedback control of integrated process networks. *Ind Eng Chem Res*. 2004;43:3528–3538.
5. Kiss AA, Bildea CS, Dimian AC, Iedema PD. Design of recycle systems with parallel and consecutive reactions by nonlinear analysis. *Ind Eng Chem Res*. 2005;44:576–587.
6. Findeisen W, Bailey FN, Brdyś M, Malinowski K, Tatjewski P, Woźniak A. *Control and Coordination in Hierarchical Systems*. John Wiley and Sons; 1980.
7. Price RM, Georgakis C. Plantwide regulatory control design procedure using a tiered framework. *Ind Eng Chem Res*. 1993;32:2693.
8. Luyben ML, Tyreus BD, Luyben WL. Plantwide control design procedure. *AIChE J*. 1997;43:3161–3174.
9. Kothare MV, Shinnar R, Rinard I, Morari M. On defining the partial control problem: concepts and examples. *AIChE J*. 2000;46:2456–2474.
10. Stephanopoulos G, Ng C. Perspectives on the synthesis of plantwide control structures. *J Proc Contr*. 2000;10:97–111.
11. Maarleveld A, Rijnsdorp JE. Constraint control on distillation columns. *Automatica*. 1970;6:51–58.
12. Luyben WL, Tyréus BD, Luyben ML. *Plantwide process control*. McGraw-Hill; 1998.
13. Larsson T, Govatsmark MS, Skogestad S, Yu CC. Control structure selection for reactor, separator, and recycle processes. *Ind Eng Chem Res*. 2003;42:1225–1234.